Research Square

Preprints are preliminary reports that have not undergone peer review.
They should not be considered conclusive, used to inform clinical practice,
or referenced by the media as validated information.

Haemorrhagic fever with renal syndrome across three endemic clusters in Jiangxi Province, China's middle Yangtze River region: long-term epidemiology and population-level changes after vaccination-programme initiation in Cluster I

Zifen Li
Jiangxi Provincial Center for Disease Control and Prevention
Huanhong Pan
Jiangxi Provincial Center for Disease Control and Prevention
Jie Liu
Jiangxi Provincial Center for Disease Control and Prevention
Tianchen Zhang
jorangezhang@163.com
Jiangxi Provincial Center for Disease Control and Prevention
Rui Gao
School of Public Health, Jiangxi Medical College, Nanchang University
Guanghui Xia
Jiangxi Provincial Center for Disease Control and Prevention
Zhili Zeng
Jiangxi Provincial Center for Disease Control and Prevention
Chenwei Li
Jiangxi Provincial Center for Disease Control and Prevention
Meiqin Huang
Jiangxi Provincial Center for Disease Control and Prevention
Tong Luo
Jiangxi Provincial Center for Disease Control and Prevention
Chengyu Li
Jiangxi Provincial Center for Disease Control and Prevention
Xiaoqing Liu
Jiangxi Provincial Center for Disease Control and Prevention
Shiyu Liao
School of Public Health, Jiangxi Medical College, Nanchang University

Shiwen Liu
Jiangxi Provincial Center for Disease Control and Prevention
Jianxiong Li
Jiangxi Provincial Center for Disease Control and Prevention

Research Article

Keywords: haemorrhagic fever with renal syndrome, age–period–cohort analysis, vaccination programme, endemic clusters

Posted Date: September 9th, 2026

DOI: https://doi.org/10.21203/rs.3.rs-10782783/v1

License: This work is licensed under a Creative Commons Attribution 4.0 International License.
Read Full License

Additional Declarations: No competing interests reported.

Abstract

Background

Haemorrhagic fever with renal syndrome (HFRS) remains an important public-health concern in endemic rural areas of China. Jiangxi contains three recognized endemic clusters, but their long-term temporal and age-related profiles, and the population-level changes following vaccination-programme initiation, have not been fully characterized.

Methods

We conducted a retrospective ecological study of HFRS surveillance records and county-level population denominators for 28 county-level units in Jiangxi from 2005 to 2024. We compared disease burden and seasonality across clusters, estimated long-term trends with Joinpoint regression, and characterized age–period–cohort (APC) patterns with an intrinsic-estimator model. In Cluster I, we used a staggered difference-in-differences design to examine changes in the incidence slope after county vaccination-programme initiation, incorporating rodent-surveillance data and sensitivity analyses of inference, functional form, treatment-effect heterogeneity, and county dependence.

Results

Across the three clusters, 7,570 cases were reported (crude incidence, 3.17 per 100,000). Cluster I had the highest burden (crude incidence, 7.00 per 100,000; age-standardized incidence rate [ASIR], 6.29). All clusters had bimodal seasonality. Joinpoint regression showed an initial rise followed by a decline; the full-period reduction was significant only in Cluster I (AAPC, − 4.28%; $P < 0.001$). APC analysis showed recent period deviations in all clusters, whereas cohort patterns were weaker and most evident in Cluster I. In Cluster I, the preferred model estimated a − 0.72 per 100,000 annual change in the incidence slope after programme initiation (95% CI, − 1.08 to − 0.35; bootstrap $P = 0.040$). Event-study estimates showed no clear pre-adoption divergence and a late reduction among the earliest adopting counties.

Conclusions

HFRS incidence varied sharply across the three endemic clusters and declined late in the study period, most clearly in Cluster I. The post-initiation slope reduction in Cluster I was compatible with a population-level programme association in the approximate target-age group, but the ecological design cannot separate programme-specific changes from concurrent calendar-time changes or estimate individual vaccine effectiveness. Risk-stratified prevention should combine vaccination, rodent-reservoir control, seasonal preparedness, and continued cluster-specific surveillance.

Background

HFRS is a rodent-borne zoonosis caused by orthohantaviruses; people are infected mainly through contact with contaminated rodent excreta. China reports more HFRS than any other country, yet risk is uneven across regions and population groups [1–7]. In endemic rural settings, the public-health response must account for differences in reservoir ecology, land use, occupation, household conditions, access to care, and prevention. A single provincial average can therefore obscure the variation needed to target surveillance and prevention resources.

Jiangxi, in the middle reaches of the Yangtze River, is an important HFRS-endemic province. Earlier county-level work identified three spatial clusters and a bimodal seasonal pattern [8]. Studies in Zhejiang, Hubei, and elsewhere in Jiangxi have reported similar spatial-temporal variation and links with meteorological or host factors [9–12]. What remains unclear is whether the three Jiangxi clusters also differ in age composition, calendar-period effects, and birth-cohort patterns—differences that would matter for targeting prevention.

An APC analysis allows these time scales to be examined together. Age patterns may reflect age-specific susceptibility or exposure; period patterns capture changes shared within a calendar period; and cohort patterns may reflect the accumulated experience of people born in different years. Jiangxi also changed rapidly during 2005–2024, with urbanization and rural–urban migration occurring alongside changes in vaccination, rodent control, surveillance, and clinical management. Because those contextual factors were not measured here, the period component is treated as a composite calendar-time pattern rather than a causal estimate of urbanization or vaccination [13, 14].

These gaps have direct implications for prevention planning. Few studies have described age, period, and birth-cohort patterns across the Jiangxi clusters; the population-level changes following county vaccination-programme initiation have not been evaluated with a staggered-adoption design in these clusters, despite earlier work in Yichun [15]; and the value of combining cluster-specific surveillance with programme evaluation has rarely been examined within one ecological framework.

We analysed routine HFRS surveillance data from Jiangxi collected between 2005 and 2024. We used the Sat Scan-based delineation reported by Yang et al. [8] to define three endemic clusters (I–III). We then combined descriptive epidemiology, age-specific Joinpoint regression, and intrinsic-estimator APC analysis to identify differences relevant to risk-stratified prevention. In Cluster I, a multi-period DID model incorporating rodent host carriage rates was used to estimate changes in incidence slope associated with vaccination-programme initiation. The analysis concerns a population-level programme association, not individual vaccine effectiveness.

Methods

2.1 Data source

We used HFRS case records from the Chinese Information System for Disease Control and Prevention (CISDCP), including laboratory-confirmed and clinically confirmed cases reported from 2005 through 2024. County assignment followed the current residential address, and calendar year was defined by illness onset. Age and sex were complete; occupations recorded as unknown were grouped with other occupations. County-level denominators by year and five-year age group were retrieved from the Public Health Science Data Center (PHSDC) search interface. All records were de-identified. The study was approved by the Ethics Review Committee of the Jiangxi Provincial Center for Disease Control and Prevention (approval no. Gan CDC Ke Lun Shen (2025) No. 04), which waived individual informed consent. The RHCR series was analysed as aggregated secondary data from routine rodent surveillance; no additional animal procedures were conducted for the present study.

2.2 Study area and cluster definition

We used the three spatiotemporal clusters identified in the earlier Jiangxi analysis [8]. They comprise 28 county-level units: Cluster I, centred on Yichun and with the highest incidence; Cluster II, around Shangrao; and Cluster III, around Fuzhou. The present study extends the observation period to 2005–2024 and stratifies the descriptive, trend, and APC analyses by cluster. Counties outside these clusters were excluded. Their geographic extent and composition are shown in Fig. 1.

Legend: Clusters I (high incidence, centred on Yichun), II (moderate incidence, around Shangrao), and III (low incidence, around Fuzhou) span 28 county-level units during 2005–2024 [8].

2.3 Statistical analysis

Incidence was expressed per 100,000 person-years. To account for differences in age structure, comparisons across clusters and years used directly standardized incidence rates with the Segi world and China 2000 standard populations. The tables and figures present Segi-standardized rates; China 2000-standardized rates are provided for reference. Rates within a single age band were left crude because standardization is not meaningful within one band. We compared sex, age-group, and occupation distributions with chi-square tests. Seasonality was summarized as a seasonal index (SI; observed/expected uniform monthly cases × 100; values above 100 indicate excess), and subgroup-specific monthly case density was shown with kernel-density plots.

We used Joinpoint regression for long-term trends. For each cluster, the overall model was fitted to the ASIR series; age-stratified models used age-specific rates. The models used a Poisson log-rate specification with mid-year population as the offset. The weighted Bayesian information criterion selected the number of joinpoints, with a maximum of three. We report annual and average annual percentage changes with 95% confidence intervals; an interval excluding zero was treated as statistically significant [16, 17].

Age, period, and cohort patterns were estimated with the web-based intrinsic-estimator APC tool. The data comprised 18 five-year age groups and four five-year calendar periods, with birth cohorts defined by period minus age. Because the three dimensions are linearly dependent, the intrinsic estimator imposes

a model-specific constraint and returns one identified descriptive representation rather than a unique causal decomposition [18–20]. We therefore interpret the deviations and rate ratios as patterns in the surveillance data, not as separate causal effects of age, calendar period, or birth cohort.

2.4 Multi-period difference-in-differences analysis after vaccination-programme initiation

We evaluated changes in HFRS incidence after county vaccination-programme initiation with a staggered-adoption DID design. The analysis was restricted to Cluster I, the only cluster with both programme-adoption and rodent-surveillance data, and to ages 15–59 years. This band approximates the stated 16–60-year target range and matches the available five-year denominators. Shanggao, Yifeng, and Gao'an initiated vaccination in 2009; Anyi and Fengxin in 2013; Xinjian in 2015; and Jing'an in 2017. Wuning was never vaccinated and served as the internal comparison county. Models 1, 2, and 4 used ages 15–59 years; Model 3 pooled the 0–14, 15–59, and ≥ 60-year strata.

We specified a linear two-way fixed-effects model:

$$Incidence_{it} = \beta_0 + \beta_1 Vacc_{it} + \beta_2 Time_t + \beta_3(Vaccination \times Time)_{it} + \gamma RHCR_t + \alpha_i + \delta_a + \varepsilon_{it}$$

In this notation, $Incidence_{it}$ is HFRS incidence per 100,000 population; $Vacc_{it}$ marks the post-adoption period; $Time_t$ is a common calendar-year trend; and Vaccination × Time is the change in the incidence slope associated with programme initiation. $RHCR_t$ is the regional annual rodent hantavirus carriage rate, α_i are county fixed effects, and δ_a are age-stratum fixed effects. Models 1–3 included county fixed effects and a common linear time trend. Model 3 pooled the 0–14, 15–59, and ≥ 60-year strata in a balanced county–age-stratum–year panel and added age-stratum fixed effects, so its coefficient is a common effect across strata rather than a population-weighted all-age rate. Model 4 added year fixed effects, which absorb the common linear trend. Model 1 was preferred because it used the approximate target-age band and included the regional rodent-surveillance covariate. RHCR came from annual antigen surveillance of rodents captured in Gao'an County from 2005 through 2024. Each annual value was the number of antigen-positive rodents divided by the number tested, multiplied by 100; zero therefore indicates completed testing with no positive specimen, not missing data. The same value was applied to all eight Cluster I counties in that year.

We estimated dynamic changes with relative-year indicators, using rel = − 1 as the reference and examining rel = − 5 to + 15. Because staggered adoption and heterogeneous effects complicate conventional event-study coefficients, these estimates were treated as descriptive and supplemented with the Callaway–Sant'Anna estimator, which uses group-time effects and not-yet-treated controls [21–27]. The age-shift literature also provides context for the age-stratified interpretation [28, 29]. We reported the Goodman–Bacon decomposition, a population-offset Poisson model, wild cluster bootstrap-t inference for the eight counties, negative-control analyses in non-target age bands, and leave-one-county-out estimates. The supporting files contain the coefficients and diagnostics for these analyses.

The provincial HFRS immunisation programme targets residents aged 16–60 years; throughout the analysis, the 15–59-year group is therefore described as an approximate target-age analytic band rather than an exact measure of vaccination eligibility or coverage.

Only eight counties contributed to the programme-effect analysis, so conventional cluster-robust inference may be unstable. We therefore used a wild cluster bootstrap-t with Webb six-point weights and 9,999 replications as the preferred inference for the slope-change estimate, while also reporting conventional county-clustered standard errors. A population-offset Poisson model tested the sensitivity of the functional form and constrained fitted incidence to non-negative values. The 95% confidence intervals for the linear coefficients are conventional cluster-robust intervals; wild-bootstrap P-values are reported separately. Analyses used R 4.6.1 with fixest 0.14.2, did 2.5.1, bacondecomp 0.1.1, readxl 1.5.0, ggplot2 4.0.3, and sandwich 3.1.2. Supporting outputs are provided in Additional files 1–6 (Tables S1–S6) and Additional files 7–12 (Figures S1–S6).

2.5 Use of AI-assisted technologies

During manuscript preparation, an AI language model was used to improve English expression and document organization. All suggestions were reviewed, verified against the source data and references, and edited by the authors, who take full responsibility for the final content.

Results

3.1 Epidemiological and demographic characteristics of HFRS cases in the three clusters

The three clusters accounted for 7,570 reported HFRS cases during 2005–2024 (Table 1). Cluster I carried the greatest burden: 4,709 cases, a crude incidence of 7.00 per 100,000, and an ASIR of 6.29. Cluster II had 1,486 cases (crude incidence 2.43; ASIR 2.03), and Cluster III had 1,375 cases (crude incidence 1.25; ASIR 1.09). Cluster I's crude incidence was about 2.9 times that of Cluster II and 5.6 times that of Cluster III; the corresponding ASIR ratios were 3.1 and 5.8. It also had the highest case-fatality rate (1.51%), followed by Cluster III (0.95%) and Cluster II (0.20%).

Clusters I, II, and III correspond to the three spatiotemporal clusters identified by Yang et al. [8].

Men accounted for 66.5%–69.7% of cases across clusters, with an overall male-to-female ratio of 2.07. The difference in sex composition was statistically significant but modest ($\chi^2 = 6.14$, $P = 0.046$). Age composition differed more clearly ($\chi^2 = 112.16$, $P < 0.001$): people aged 15–59 years made up 67.1%–74.3% of cases, while Cluster I had the largest share of children aged 0–14 years (10.7%) and the smallest share of adults aged 60 years or older (22.1%); Cluster II had the largest elderly share (26.2%) and Cluster III an intermediate one (20.4%). Farmers represented 66.4%–69.9% of cases in each cluster (overall $\chi^2 = 112.06$, $P < 0.001$); students were more common in Cluster I (11.7%).

Age standardization did not remove the incidence gradient (Table 2). Cluster I remained highest overall and in both sexes (overall ASIR 6.29; male 8.03; female 4.39). Within every cluster, men had higher ASIRs than women. Adults aged 60 years or older had the highest age-specific rate in each cluster (11.71, 4.73, and 2.06 per 100,000 in Clusters I–III), while the 0–14-year group had the lowest. The same cluster and sex patterns were obtained with the China 2000 standard population (Table 2, Note).

Table 1
Demographic characteristics and HFRS burden across endemic clusters.

Characteristic	Cluster I	Cluster II	Cluster III	Total	χ^2	P-value
Cases, n (incidence per 100 000)	4709 (7.00)	1486 (2.43)	1375 (1.25)	7570 (3.17)		
Deaths, n (CFR, %)	71 (1.51)	3 (0.20)	13 (0.95)	87 (1.15)		
Gender, n (%)					6.14	0.046
Male	3130 (66.47)	1035 (69.65)	943 (68.58)	5108 (67.48)		
Female	1579 (33.53)	451 (30.35)	432 (31.42)	2462 (32.52)		
Male: female ratio	1.98	2.29	2.18	2.07		
Age group, n (%)					112.16	< 0.001
0–14	505 (10.72)	50 (3.36)	73 (5.31)	628 (8.30)		
15–59	3162 (67.15)	1047 (70.46)	1022 (74.33)	5231 (69.10)		
60+	1042 (22.13)	389 (26.18)	280 (20.36)	1711 (22.60)		
Occupation, n (%)					112.06	< 0.001
Farmers	3151 (66.91)	1038 (69.85)	913 (66.40)	5102 (67.40)		
Housework/unemployment	318 (6.75)	153 (10.30)	118 (8.58)	589 (7.78)		
Students	552 (11.72)	68 (4.58)	86 (6.25)	706 (9.33)		
Others	688 (14.61)	227 (15.28)	258 (18.76)	1173 (15.50)		

Note: Values are n (%) unless otherwise specified. Incidence is per 100 000 person-years. Clusters I, II, and III correspond to the three spatiotemporal clusters identified by Yang et al. [8]. The chi-square/P values in the Gender, Age group, and Occupation header rows compare the full categorical distributions across clusters. Case-fatality-rate values are descriptive, and no formal case-fatality-rate comparison is reported.

Table 2
Age-standardized HFRS incidence rates across endemic clusters.

Characteristic	Cluster I	Cluster II	Cluster III	Total
Overall	6.29	2.03	1.09	2.80
Male	8.03	2.78	1.45	3.66
Female	4.39	1.27	0.71	1.88
Age 0–14 (age-specific)	3.76	0.38	0.31	1.26
Age 15–59 (age-specific)	7.04	2.62	1.40	3.31
Age 60+ (age-specific)	11.71	4.73	2.06	5.57

Note: Rates are per 100 000 person-years. Overall, male and female rates are age-standardized using the direct method with the Segi world standard; age-group rates are age-specific (crude) rates and are not standardized. For reference, ASIR used the China 2000 standard population: Overall 6.70 / 2.20 / 1.16 (Clusters I/II/III; Total 2.99); Male 8.62 / 3.03 / 1.58 (Total 3.95); Female 4.62 / 1.35 / 0.73 (Total 1.98). Abbreviation: ASIR, age-standardized incidence rate.

3.2 Seasonal distribution and age-stratified case density

Seasonality was bimodal in all three clusters, but the balance between peaks differed (Table 3; Fig. 2). Cluster I had a clear winter peak in December and January (SI 214.9 and 160.5) and a second peak in May and June (129.6 and 126.8). Cluster II showed the most even pattern: December and November were the main winter months (181.7 and 176.0), followed by May and June (130.8 and 134.9). Cluster III was strongly winter-dominant, with the largest primary peak (December 264.8, January 185.7) and a weak spring–summer signal (May 87.4, June 67.1). These patterns are consistent with the dual seasonal pattern reported elsewhere in China [30–32].

The second peak was not distributed evenly across subgroups (Fig. 3). It remained visible in the monthly case-density curves across age and occupation strata in Cluster I, was moderate in Cluster II, and was largely absent in Cluster III, where reported cases were concentrated in winter. The contrast may reflect differences in exposure schedules or reservoir systems, but neither host species nor individual exposure behaviour was measured in this study.

Legend: Age-standardized incidence rate trends and seasonal index of HFRS across the three endemic clusters, Jiangxi Province, China, 2005–2024.

Table 3
Seasonal index of HFRS by endemic cluster.

Cluster	Primary peak (month, SI)	Secondary peak (month, SI)	Bimodality
I	December (214.9), January (160.5)	May (129.6), June (126.8)	Clear
II	December (181.7), November (176.0)	May (130.8), June (134.9)	Most balanced
III	December (264.8), January (185.7)	Weak: May (87.4), June (67.1)	Winter-dominant
Note: Seasonal index = (observed monthly cases / expected uniform monthly cases) × 100; SI > 100 denotes excess.			

Legend: Kernel-density plots of illness-onset month among reported HFRS cases, stratified by age group, sex, and occupation across the three endemic clusters, Jiangxi Province, China, 2005–2024.

3.3 Temporal trend analysis: Joinpoint regression and age–period–cohort models

3.3.1 Long-term incidence trends identified by Joinpoint regression

Joinpoint regression showed an initial rise followed by a post-inflection decline in all three clusters. For the total age-standardized series, only Cluster I had a statistically significant full-period AAPC; age-specific analyses showed additional significant changes in the 0–14-year stratum in Cluster II and the ≥ 60-year stratum in Cluster III (Fig. 4; Table 4). The trends describe when incidence changed, not why it changed.

Age-specific trends were less uniform. Incidence in the 15–59-year group declined significantly in Cluster I and more weakly, without statistical significance, in Clusters II and III. The ≥ 60-year group had a positive AAPC in every cluster, reaching statistical significance in Cluster III. Because vaccination coverage and other age-specific exposures were not observed, these differences should not be read as evidence of vaccine effectiveness. Detailed segment-specific Joinpoint and AAPC estimates are provided in Additional file 1.

Legend: Open circles show observed annual rates; solid lines show Joinpoint fitted trends; and shaded ribbons show 95% confidence intervals. Age-standardized incidence is shown for the total population and age-specific incidence for the three age groups, Jiangxi Province, China, 2005–2024.

Table 4
Average annual percentage change in HFRS incidence by cluster and age group.

Population subgroup	Cluster I	Cluster II	Cluster III
Total (age-standardized)	−4.28 (− 7.27, − 2.18)*	−2.54 (− 7.08, + 1.57)	−0.32 (− 6.41, + 4.22)
0–14 years	−3.46 (− 8.87, + 0.39)	−5.99 (− 11.96, − 2.96)*	−0.69 (− 15.45, + 18.27)
15–59 years	−5.64 (− 9.45, − 3.45)*	−2.39 (− 5.39, + 1.06)	−0.64 (− 8.35, + 4.52)
≥ 60 years	+ 1.69 (− 0.85, + 5.10)	+ 2.33 (− 2.61, + 9.98)	+ 6.29 (+ 1.59, + 15.76)*

Note: AAPC computed as 100 × (e^β − 1); 95% confidence intervals shown in parentheses. * Statistically significant at P < 0.05. Positive AAPC denotes rising incidence. Cluster I, II, and III denote the three HFRS aggregation areas identified by SaTScan space–time scan [8]. Source data: Chinese Information System for Disease Control and Prevention (CISDCP). Abbreviation: AAPC, average annual percentage change.

3.3.2 Age–period–cohort effects

The age effect differed in shape between the three clusters (Fig. 5 and the supporting figures), reflecting cluster-specific age patterns of infection risk that are not captured by the period and cohort summaries alone; the complete age-specific incidence curves are plotted there.

The age component also differed by cluster. Cluster I had a bimodal age-incidence profile, with a pronounced early-adolescent peak (largest positive deviation at approximately 12.5 years) and a high absolute rate among older adults, as shown in Figure S1 (Additional file 7), together with a relative deficit at ages 55–65 years. Clusters II and III were unimodal and centred on middle age: Cluster II peaked later, at approximately 42.5 years, and declined more sharply in old age; Cluster III peaked at approximately 32.5 years and declined more gradually. Across clusters, the lowest relative risk occurred in early childhood (approximately 2.5 years), most strongly in Cluster II (deviation − 1.80).

Period effects accounted for the largest relative deviations in all three clusters, including a significant decline in 2022.5. A period effect can reflect several changes occurring at the same time—reservoir dynamics, prevention and surveillance, social conditions, clinical management, or vaccination. In Cluster I, the decline overlaps with the estimated programme-effect slope change. In Clusters II and III, no vaccination-programme effect was estimated, so their period declines cannot be attributed to vaccination. The corresponding period rate ratios are reported in Table 5.

Cohort effects were weaker. Overall statistical significance was reached only in Cluster I, suggesting that generation-specific differences in recorded HFRS risk were limited in Clusters II and III.

Legend: Intrinsic-estimator APC effects for the three clusters. Panels A–C, D–F, and G–I correspond to Cluster I (red), Cluster II (green), and Cluster III (blue), respectively. Each row shows deviations of age,

period, and cohort effects from the reference, with 95% confidence intervals and a dashed line at zero.

Table 5
APC period rate ratios of HFRS by endemic cluster.

Cluster	Period RR 2007.5 (95% CI)	Period RR 2017.5 (95% CI)	Period RR 2022.5 (95% CI)
I	0.81 (0.72–0.91)	1.06 (0.95–1.18)	0.48 (0.42–0.56)
II	0.71 (0.60–0.84)	1.01 (0.88–1.17)	0.71 (0.59–0.84)
III	0.57 (0.48–0.69)	1.23 (1.07–1.43)	0.64 (0.53–0.77)

Note: Estimates from the NCI web-based APC tool (intrinsic estimator; reference period 2012.5 = 1.00). All three clusters showed a statistically significant period-effect decline in 2022.5; Cluster III showed a significant elevation in 2017.5. Abbreviations: RR, rate ratio; NCI, National Cancer Institute.

The corresponding age-specific incidence curves and period and cohort rate ratios are provided in Figure S2 (Additional file 8) and Table S1 (Additional file 1).

3.4 Vaccination-programme initiation and HFRS incidence

In the preferred Cluster I specification, vaccination-programme initiation was associated with a − 0.72 per 100,000 annual change in the incidence slope (95% CI − 1.08 to − 0.35; nominal cluster-robust $P < 0.01$; Table 6). The coefficient remained negative without RHCR (− 0.82; 95% CI − 1.29 to − 0.34; nominal cluster-robust $P < 0.05$), in the pooled three-age-stratum model (− 0.81; 95% CI − 1.23 to − 0.38; nominal cluster-robust $P < 0.01$), and with year fixed effects, although the last estimate was smaller. RHCR was positive but imprecisely estimated, and its separate ecological time-series showed the same direction without statistical significance. These estimates are compatible with a programme-level association, but they do not separate vaccination from reservoir dynamics or other calendar-time changes. The event-study estimates underpinning the preferred specification are plotted in Fig. 6.

The sensitivity analyses pointed in the same direction, although the estimates address different questions. Wild cluster bootstrap-t inference supported a negative slope change in the preferred and no-RHCR specifications ($P = 0.040$ and 0.032). The population-offset Poisson model estimated an incidence-rate ratio of 0.92 per post-adoption year (95% CI 0.86–0.98; $P = 0.015$), while the Callaway–Sant'Anna estimator gave an ATT of − 4.00 per 100,000 (95% CI − 6.62 to − 1.37; $P < 0.01$). Neither quantity is the same estimand as the − 0.72 annual slope change. Negative-control estimates were non-significant in the ≥ 60-year group (− 1.05; $P = 0.087$) and the 0–14-year group (− 0.33; $P = 0.120$). They therefore did not establish target-age specificity and remained compatible with shared period effects or spillover. The late relative-year reductions were driven mainly by the earliest-adopting counties and should not be treated as a common delay for every adoption cohort. Goodman–Bacon, placebo, and leave-one-county-out results were used as corroborative diagnostics rather than independent evidence.

Additional files 2–6 and 9–12 contain the relative-year coefficients, RHCR analysis, counterfactual trajectory, Goodman–Bacon decomposition, Callaway–Sant'Anna estimates, placebo analyses, and

leave-one-county-out results (Tables S2–S6 and Figures S3–S6). The APC figures and tables are listed separately in the Additional files section.

Legend: Incidence (per 100,000) in Cluster I (eight counties), Jiangxi Province, 2005–2024. Panel A: preferred specification (ages 15–59 years, adjusted for rodent carriage rate). Panel B: ages 15–59 years without rodent control. Panel C: pooled age-stratum specification (0–14, 15–59, and ≥ 60 years) with age-stratum fixed effects. Panel D: ages 15–59 years with year fixed effects. Shaded area: pre-implementation period (rel < 0). Dashed vertical line: rel = 0. Error bars: 95% confidence intervals with county-clustered standard errors. The y-axis shows the difference in incidence relative to rel = − 1.

Table 6
Difference-in-differences estimates following vaccination-programme initiation.

	(1)	(2)	(3)	(4)
	Ages 15–59 years + rodent rate (preferred)	**Ages 15–59 years**	**Pooled age strata (0–14, 15–59, ≥ 60)**	**Ages 15–59 years + year FE**
Vaccination program (level)	8.234* (2.490)	9.086* (2.777)	7.948** (1.729)	4.542† (2.186)
Time (annual trend)	0.057 (0.126)	0.151 (0.176)	0.223 (0.165)	—
Vaccination × Time (slope change)	-0.718** (0.187)	-0.815* (0.236)	-0.808** (0.180)	-0.445† (0.205)
Rodent carriage rate (RHCR)	0.373† (0.166)	—	—	—
County fixed effects	Yes	Yes	Yes	Yes
Age-stratum fixed effects	No	No	Yes	No
Year fixed effects	No	No	No	Yes
County-clustered SE	Yes	Yes	Yes	Yes
Observations	160	160	480	160

Note: Staggered-adoption difference-in-differences models. The outcome is HFRS incidence per 100 000 population. Models 1–3 include county fixed effects and a common linear time trend. Model 3 additionally pools the 0–14, 15–59, and ≥ 60-year strata and includes age-stratum fixed effects; Model 4 additionally includes year fixed effects, which absorb the common linear trend. Model 1 is preferred and is restricted to the 15–59-year analytic band that approximates the programme target range; this band is not a direct measure of vaccination coverage. Vaccination × Time is the programme-effect change in the incidence slope. The vaccination-programme level term is a pre–post mean shift and is not the estimand of interest. Model 3 contains 480 observations (8 counties × 20 years × 3 age strata). † P < 0.10, * P < 0.05, ** P < 0.01, *** P < 0.001.

Discussion

4.1 Descriptive epidemiology and disease burden

Across the 20-year series, Cluster I carried the greatest HFRS burden (crude incidence 7.00 per 100,000; ASIR 6.29) and the highest case-fatality rate (1.51%). Its incidence gradient persisted after age standardization, so differences in age structure alone cannot explain the contrast between clusters. The

predominance of men and farmers is compatible with occupational and peridomestic exposure to rodents, although aggregated surveillance data cannot distinguish exposure intensity from differences in healthcare seeking or reporting. Most cases occurred at ages 15–59 years, but adults aged 60 years or older had the highest age-specific rate in every cluster. Prevention planning should distinguish the working-age groups that contributed most reported cases from older residents with the highest age-specific rates, rather than rely on a uniform provincial response.

4.2 Seasonal heterogeneity and its implications

Seasonality also separated the clusters. All three had a winter peak and a smaller spring–summer peak, but the second peak was much weaker in Cluster III. The contrast is consistent with different exposure rhythms or reservoir systems, yet the study did not measure virus type, rodent species, meteorological variables, or individual behaviour. A bimodal pattern does not by itself require two co-circulating hantavirus species. In Shaanxi, Hantaan virus contributes substantially to HFRS burden [33], while a molecular study in Xi'an detected Hantaan virus in sampled rodents and patients but no Seoul virus [34]. HFRS nevertheless showed both autumn–winter and spring–summer peaks [33]. Hantaan virus has also been isolated from outdoor *Apodemus agrarius* in Jiangxi [35]. Seasonal field work may contribute to the second peak, but this remains a hypothesis because farming calendars, land use, individual exposure, virus type and rodent species were not measured. The timing of the peaks is therefore a useful surveillance signal, not evidence for a specific hantavirus mechanism.

4.3 Temporal trends, age–period–cohort patterns, and prevention planning

The long-term analyses answer different questions. Joinpoint regression describes the direction and timing of changes, while APC analysis shows how those changes are distributed across age, period, and cohort. Both indicated substantial recent-period variation, but neither identifies its cause. The period component may combine reservoir dynamics, prevention, surveillance, social conditions, clinical management, and vaccination. Urbanization and rural–urban migration are plausible influences, but they were not measured here [13, 14]. For public-health planning, the period patterns should therefore be used to guide surveillance and intervention timing, not to assign changes to one programme component.

The age deviations are useful for generating prevention hypotheses, not for assigning mechanisms. The early-adolescent peak in Cluster I and the middle-age profiles in Clusters II and III could reflect differences in household, school, or agricultural exposure, but those exposures were not recorded. The low relative risk in early childhood and the high absolute rates among older adults suggest priorities for surveillance. Testing these explanations will require age- and cluster-specific exposure histories, serology, and rodent data.

4.4 Interpretation of the association after vaccination-programme initiation

The preferred 15–59-year Cluster I model showed a − 0.72 per 100,000 annual change in the incidence slope after programme initiation (95% CI − 1.08 to − 0.35). Model 3, which pooled the 0–14, 15–59, and ≥ 60-year strata, produced a similar estimate (− 0.81; 95% CI − 1.23 to − 0.38; P = 0.003), although its common slope change across age strata is not an age-specific vaccine-effect estimate. The preferred coefficient remained negative under wild cluster bootstrap-t inference (P = 0.040). A recent meta-analysis of inactivated HFRS vaccine studies supports protective efficacy [36], and an observational study in Hu County reported a population-level association [37]. Our county-year ecological analysis should be read as a programme-level association, not as individual vaccine effectiveness or definitive causal evidence.

The event-study results showed no clear pre-adoption divergence, while reductions appeared mainly at relative years 12–15 in the primary 15–59-year specification. Those late coefficients were identified largely from the earliest-adopting counties, so they should not be interpreted as a uniform delay across cohorts. Gradual accumulation of population-level protection, incomplete uptake, changing age composition, waning immunity, reservoir dynamics [38], and other period changes could all contribute; the design cannot distinguish among them. The negative-control estimate was − 1.05 in the ≥ 60-year group (P = 0.087) and − 0.33 in the 0–14-year group (P = 0.120); both were imprecise and non-significant. Shared secular change and spillover therefore remain possible. Vaccination and rodent-reservoir control should be considered together while the timing and mechanism of the association are investigated further.

The programme analyses estimate different quantities. The preferred linear model estimates a change in incidence slope; the Poisson model estimates a rate ratio per year; and the Callaway–Sant'Anna model summarizes group-time treatment effects. Their directions were broadly similar, but the estimates are not interchangeable. The Goodman–Bacon decomposition showed that conventional TWFE weighting was affected by heterogeneous-treatment-effect comparisons, including negative-weight comparisons, and leave-one-county-out estimates varied in size while remaining negative. The overall pattern is compatible with a beneficial programme association, but the small number of counties, one never-treated comparison county, treatment-effect heterogeneity, and possible time-varying confounding prevent a definitive causal conclusion.

These findings support a stratified prevention approach rather than a uniform provincial response. Cluster I warrants intensified integrated prevention because it had the greatest burden, whereas the differences in age composition and seasonal patterns across clusters can guide local surveillance and health education. Older adults merit particular attention because they had the highest age-specific rates in every cluster. The Cluster I analysis supports continued evaluation of vaccination-programme delivery alongside local coverage data, rodent surveillance, and measures of other concurrent prevention activities. This framework may help other endemic rural settings use routine surveillance to align vaccination, rodent control, and case-based monitoring, but it requires local validation before direct adoption elsewhere.

4.5 Public health implications

4.6 Study limitations

Several limitations should be weighed against these findings.

The vaccination programme was a natural experiment rather than a randomized trial. The DID design relies on parallel trends and cannot rule out time-varying confounders shared across counties, including rodent-control campaigns, changes in prevention and control policies [39], and the COVID-19 period; inference rests on only eight counties and one never-treated comparison county. Individual vaccination histories and county-level coverage were unavailable, and the 15–59-year analysis band only approximated the 16–60-year programme target. The estimate should therefore be read as a programme-level association rather than individual vaccine effectiveness.

The DID analysis covered only Cluster I and used a regional RHCR series from one sentinel county. Findings may therefore not generalize to Clusters II and III, other provinces, or different ecological settings. Hantavirus species were not typed for the cases analysed here, so the contributions of *Apodemus*- and *Rattus*-associated transmission to the two seasonal peaks could not be separated.

Conclusions

From 2005 to 2024, HFRS in Jiangxi showed a strong cluster gradient, shared bimodal seasonality, and a late-period decline that was clearest in Cluster I. APC analysis pointed to prominent recent-period changes and weaker, cluster-specific cohort patterns. In Cluster I, vaccination-programme initiation was associated with a reduction in the incidence slope in the approximate target-age band, with the signal appearing late; the pooled age-stratum model gave a similar estimate (− 0.81; 95% CI − 1.23 to − 0.38). This remains an ecological programme-level association, not a measure of individual vaccine effectiveness or a definitive causal effect.

The practical implication is a risk-stratified prevention strategy: vaccination, rodent-reservoir surveillance and control, seasonal preparedness, continued attention to older adults and other high-rate groups, and planning that reflects cluster-specific risk. Cluster I, with the greatest burden, warrants particular attention, while all clusters require prevention timed to their local seasonal patterns. Studies with individual vaccination histories and county-level coverage, direct measures of urbanization and land use, broader reservoir surveillance with virus typing, and seasonal exposure data linked to agricultural calendars are needed to separate programme associations from concurrent ecological and calendar-time changes.

Abbreviations

HFRS
haemorrhagic fever with renal syndrome

CISDCP
Chinese Information System for Disease Control and Prevention
PHSDC
Public Health Science Data Center
ASIR
age-standardized incidence rate
APC
age–period–cohort (model)
AAPC
average annual percentage change
NCI
National Cancer Institute
wBIC
weighted Bayesian information criterion
DID
difference-in-differences
TWFE
two-way fixed effects
ATT
average treatment effect on the treated
RHCR
rodent hantavirus carriage rate
SI
seasonal index
CFR
case-fatality rate
RR
rate ratio
CI
confidence interval.

Declarations

Ethics approval and consent to participate

This study was a retrospective analysis of aggregated, de-identified notifiable-disease surveillance records and publicly available demographic data; no individually identifiable information was accessed at any stage. HFRS is a statutorily notifiable infectious disease in China, and its surveillance data are routinely collected through the Chinese Information System for Disease Control and Prevention (CISDCP) under the Law of the People's Republic of China on the Prevention and Treatment of Infectious Diseases.

The study protocol was reviewed and approved by the Ethics Review Committee of the Jiangxi Provincial Center for Disease Control and Prevention (approval no. Gan CDC Ke Lun Shen (2025) No. 04). Because the analysis used only anonymized, aggregated secondary data and posed no more than minimal risk to participants, the requirement for individual informed consent was waived by the same committee. All methods were performed in accordance with the relevant guidelines and regulations and with the principles of the Declaration of Helsinki. The RHCR series was analysed as aggregated secondary data from routine rodent surveillance; no additional animal procedures were conducted for this study, and animal ethics approval was therefore not applicable to this secondary analysis.

Consent for publication

Not applicable. This manuscript does not contain any data or images relating to an identifiable individual person.

Availability of data and materials

The datasets generated and/or analyzed during the current study are not publicly available because of national data-governance and privacy restrictions, but aggregated, de-identified data are available from the corresponding author on reasonable request, subject to permission from the relevant health authority. Age- and region-stratified population denominators are publicly available from the PHSDC [40]. The analytical R scripts are available from the corresponding author on reasonable request.

Competing interests

The authors declare that they have no competing interests.

Funding

This work was supported by the National Natural Science Foundation of China [grant 8236120472 to XQL]; the Natural Science Foundation of Jiangxi Province, China [grants 20242BAB25552 to TCZ and 20252BAC240490 to JL]; Youth Science Foundation of Jiangxi Province, China [grant 20171BAB215051 to TCZ]; the Jiangxi Provincial Key Laboratory of Major Epidemic Prevention and Control [grant 2024SSY06021 to XQL]; and the Science and Technology Program of the Jiangxi Provincial Health Commission [grant 202610833 to GHX]. The funders had no role in the study design, data collection and analysis, decision to publish, or preparation of the manuscript.

Authors’ contributions

ZFL, HHP, JL, and TCZ conceived and designed the study. XQL, JXL, and SWL provided resources, including access to HFRS surveillance records and a population database, and coordinated official data use approval. RG, ZLZ, CWL, and TL curated, cleaned, and validated the surveillance and demographic data. ZFL, GHX, MQH, CYL, and SYL performed the statistical analyses (descriptive, Joinpoint, age–period–cohort, and difference-in-differences). ZFL drafted the manuscript. TCZ supervised the project and critically revised the manuscript for important intellectual content. All authors read and approved the final manuscript.

Acknowledgements

We thank the staff of the Jiangxi Provincial Center for Disease Control and Prevention and the prefecture- and county-level CDCs for their careful work in HFRS case reporting and rodent surveillance. Their routine surveillance made this analysis possible.

References

1. Watson DC, Sargianou M, Papa A, Chra P, Starakis I, Panos G. Epidemiology of Hantavirus infections in humans: a comprehensive, global overview. Crit Rev Microbiol. 2014;40(3):261–72. 10.3109/1040841X.2013.783555.
2. Wen B, Yang Z, Ren S, Fu T, Li R, Lu M, et al. Spatial-temporal patterns and influencing factors for hemorrhagic fever with renal syndrome: a 16-year national surveillance analysis in China. One Health. 2024;18:100725. 10.1016/j.onehlt.2024.100725.
3. Liu S, Zhang T. A long-term retrospective analysis of the haemorrhagic fever with renal syndrome epidemic from 2005 to 2021 in Jiangxi Province, China. Sci Rep. 2023;13:2268. 10.1038/s41598-023-29330-4.
4. Sehgal A, Mehta S, Sahay K, Martynova E, Rizvanov A, Baranwal M, et al. Hemorrhagic fever with renal syndrome in Asia: history, pathogenesis, diagnosis, treatment, and prevention. Viruses. 2023;15(2):561. 10.3390/v15020561.
5. Zhang YZ, Zou Y, Fu ZF, Plyusnin A. Hantavirus Infections in Humans and Animals, China. Emerg Infect Dis. 2010;16(8):1195–203. 10.3201/eid1608.090470.
6. Chen JJ, Guo TC, Song SX, Shao ZJ, Liu K. Epidemiological characteristics and the development of spatiotemporal analysis models on hemorrhagic fever with renal syndrome in China. Chin J Epidemiol. 2020;41(10):1735–40. 10.3760/cma.j.cn112338-20191108-00794.
7. Zheng Z, Li Z, Huang X, Wang Q, Du S, Li A, et al. Hemorrhagic fever with renal syndrome and diversity and distribution of Hantaviruses - China, 2014–2023. China CDC Wkly. 2025;7(25):858–62. 10.46234/ccdcw2025.141.
8. Yang S, Gao Y, Liu X, Liu X, Liu Y, Metelmann S, et al. Spatiotemporal dynamics of hemorrhagic fever with renal syndrome in Jiangxi province, China. Sci Rep. 2020;10:14291. 10.1038/s41598-020-70761-0.

9. Su F, Liu Y, Ling F, Zhang R, Wang Z, Sun J. Epidemiology of Hemorrhagic Fever with Renal Syndrome and Host Surveillance in Zhejiang Province, China, 1990–2021. Viruses. 2024;16(1):145. 10.3390/v16010145.
10. Wu H, Wang X, Xue M, Wu C, Lu Q, Ding Z, et al. Spatial-temporal characteristics and the epidemiology of haemorrhagic fever with renal syndrome from 2007 to 2016 in Zhejiang Province, China. Sci Rep. 2018;8:10244. 10.1038/s41598-018-28610-8.
11. Li H, Yang R, Guan X, Huang X, Jiang H, Tan L, et al. Spatiotemporal distribution and meteorological factors of hemorrhagic fever with renal syndrome in Hubei province. PLoS Negl Trop Dis. 2024;18:e0012498. 10.1371/journal.pntd.0012498.
12. Song N, Xie Y, Ding S, Liu X, Pan H, Yuan H. Analysis of spatial autocorrelation of hemorrhagic fever with renal syndrome in Jiangxi Province from 2013 to 2018. Chin J Dis Control Prev. 2020;24(8):876–80. 10.16462/j.cnki.zhjbkz.2020.08.003.
13. Tian H, Hu S, Cazelles B, Chowell G, Gao L, Laine M, et al. Urbanization prolongs hantavirus epidemics in cities. Proc Natl Acad Sci U S A. 2018;115(18):4707–12. 10.1073/pnas.1712767115.
14. Wei Q, Ren H, Lu L, Shi R. Non-negligible impacts of urbanization on spatiotemporal variations of infectious disease: a case study of hemorrhagic fever with renal syndrome epidemics in China. Infect Dis Poverty. 2025;14:104. 10.1186/s40249-025-01366-w.
15. Liu X, Zhang T, Xie C, Xie Y. Changes of HFRS incidence caused by vaccine intervention in Yichun City, China, 2005–2013. Med Sci Monit. 2016;22:295–301. 10.12659/msm.895886.
16. Kim HJ, Fay MP, Feuer EJ, Midthune DN. Permutation tests for joinpoint regression with applications to cancer rates. Stat Med. 2000;19(3):335–51. 10.1002/(SICI)1097-0258(20000215)19:3%3C335::AID-SIM336%3E3.0.CO;2-Z.
17. Clegg LX, Hankey BF, Tiwari R, Feuer EJ, Edwards BK. Estimating average annual per cent change in trend analysis. Stat Med. 2009;28(29):3670–82. 10.1002/sim.3733.
18. Yang Y, Fu WJ, Land KC. A Methodological Comparison of Age-Period-Cohort Models: The Intrinsic Estimator and Conventional Generalized Linear Models. Sociol Methodol. 2004;34(1):75–110. 10.1111/j.0081-1750.2004.00148.x.
19. Rosenberg PS, Check DP, Anderson WF. A web tool for age-period-cohort analysis of cancer incidence and mortality rates. Cancer Epidemiol Biomarkers Prev. 2014;23(11):2296–302. 10.1158/1055-9965.epi-14-0300.
20. Luo L. Assessing validity and application scope of the intrinsic estimator approach to the age-period-cohort problem. Demography. 2013;50(6):1945–67. 10.1007/s13524-013-0243-z.
21. Bertrand M, Duflo E, Mullainathan S. How much should we trust differences-in-differences estimates? Q J Econ. 2004;119(1):249–75. 10.1162/003355304772839588.
22. Sun L, Abraham S. Estimating dynamic treatment effects in event studies with heterogeneous treatment effects. J Econometrics. 2021;225(2):175–99. 10.1016/j.jeconom.2020.09.006.
23. Goin DE, Riddell CA. Comparing two-way fixed effects and new estimators for differences-in-differences: A simulation study and empirical example. Epidemiology. 2023;34(4):535–43.

10.1097/EDE.0000000000001611.

24. Goodman-Bacon A. Difference-in-differences with variation in treatment timing. J Econometrics. 2021;225(2):254–77. 10.1016/j.jeconom.2021.03.014.
25. Wing C, Yozwiak M, Hollingsworth A, Freedman S, Simon K. Designing Difference-in-Difference Studies with Staggered Treatment Adoption: Key Concepts and Practical Guidelines. Annu Rev Public Health. 2024;45:485–505. 10.1146/annurev-publhealth-061022-050825.
26. Callaway B, Sant'Anna PHC. Difference-in-differences with multiple time periods. J Econometrics. 2021;225(2):200–30. 10.1016/j.jeconom.2020.12.001.
27. Feng S, Ganguli I, Lee Y, Poe J, Ryan A, Bilinski A. Difference-in-Differences for Health Policy and Practice: A Review of Modern Methods. Stat Med. 2025;44(23–24):e70247. 10.1002/sim.70247.
28. He X, Wang S, Huang X, et al. Changes in age distribution of hemorrhagic fever with renal syndrome: an implication of China's expanded program of immunization. BMC Public Health. 2013;13:394. 10.1186/1471-2458-13-394.
29. Park Y. Epidemiologic study on changes in occurrence of hemorrhagic fever with renal syndrome in Republic of Korea for 17 years according to age group: 2001–2017. BMC Infect Dis. 2019;19:153. 10.1186/s12879-019-3794-9.
30. Lv C-L, Tian Y, Qiu Y, Xu Q, Chen J-J, Jiang B-G, et al. Dual seasonal pattern for hemorrhagic fever with renal syndrome and its potential determinants in China. Sci Total Environ. 2023;859:160339. 10.1016/j.scitotenv.2022.160339.
31. Luo Y, Lv H, Yan H, Zhu C, Ai L, Li W, et al. Meteorological change and hemorrhagic fever with renal syndrome epidemic in China, 2004–2018. Sci Rep. 2022;12:20037. 10.1038/s41598-022-23945-9.
32. Zhang WY, Wang LY, Liu YX, Yin WW, Hu WB, Soares Magalhaes RJ, et al. Spatiotemporal transmission dynamics of hemorrhagic fever with renal syndrome in China, 2005–2012. PLoS Negl Trop Dis. 2014;8(11):e3344. 10.1371/journal.pntd.0003344.
33. Liang W, Gu X, Li X, Zhang K, Wu K, Pang M, et al. Mapping the epidemic changes and risks of hemorrhagic fever with renal syndrome in Shaanxi Province, China, 2005–2016. Sci Rep. 2018;8(1):749. 10.1038/s41598-017-18819-4.
34. Ma C, Yu P, Nawaz M, Zuo S, Jin T, Li Y, et al. Hantaviruses in rodents and humans, Xi'an, PR China. J Gen Virol. 2012;93(Pt 10):2227–36. 10.1099/vir.0.043364-0.
35. Liu SW, Gong T, Xu G, Shi Y, Li JX, Zhang YN, et al. Complete genome sequence analysis of Hantaan virus strain AYW89-15 isolated in Jiangxi, China. Chin J Zoonoses. 2017;33(12):1089–93. 10.3969/j.issn.1002-2694.2017.12.007.
36. Wu W, Liu J, Guo S, Zhao H, Yang X. The protective efficacy of inactivated vaccine against hemorrhagic fever with renal syndrome: a meta-analysis. Med (Baltim). 2025;104(20):e42463. 10.1097/MD.0000000000042463.
37. Xiao D, Wu K, Tan X, Yan T, Li H, Yan Y, et al. The impact of the vaccination program for hemorrhagic fever with renal syndrome in Hu County, China. Vaccine. 2014;32(6):740–5. 10.1016/j.vaccine.2013.11.024.

38. Liu YY, Yang A, Xu YQ, Zhang YH, Bai CS, Zhang YQ, et al. Incidence of Orthohantavirus infection in humans follows observed changes in rodent reservoirs, Hubei Province, China (1984–2010). Am J Vet Res. 2023;84(8). ajvr.22.12.0215.
39. Wang Z, Wei Y, Cai Y, Zhang M, Wang Z, Han X, et al. Impact of hemorrhagic fever with renal syndrome control policies in Hebei Province: an interrupted time series analysis. BMC Infect Dis. 2026;26:459. 10.1186/s12879-026-12669-0.
40. Public Health Science Data Center. https://www.phsciencedata.cn/. Accessed 4 Aug 2026.

Figures

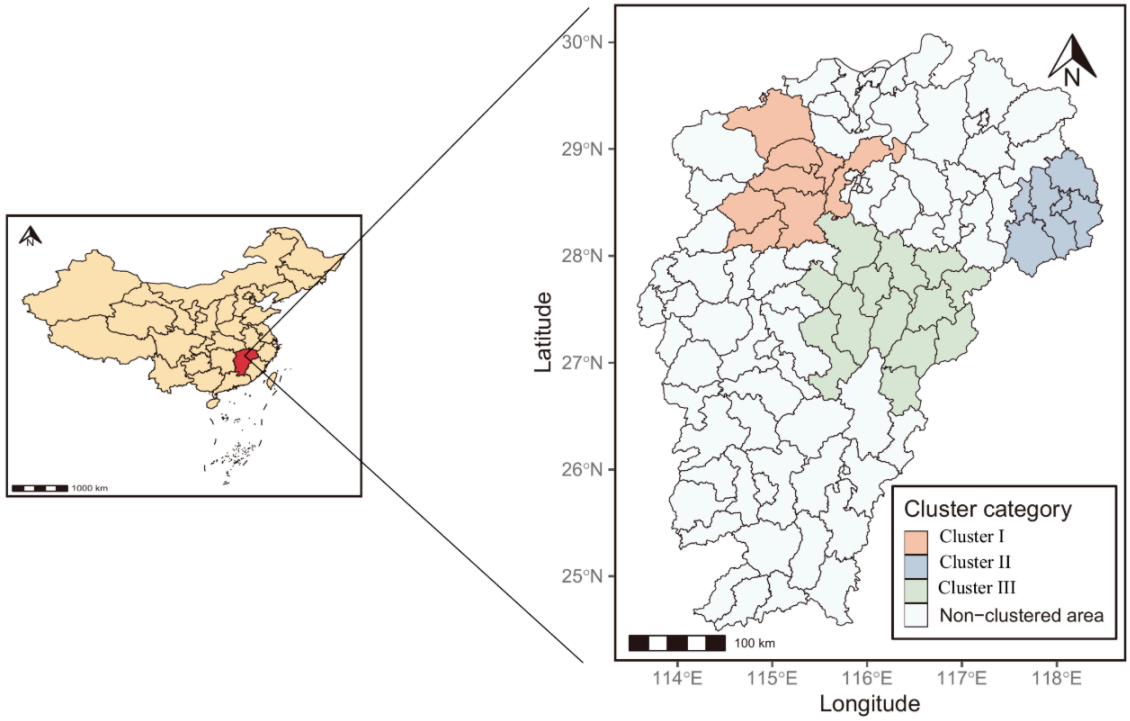


Figure 1

Geographic distribution of HFRS endemic clusters in Jiangxi Province.

Legend: Clusters I (high incidence, centred on Yichun), II (moderate incidence, around Shangrao), and III (low incidence, around Fuzhou) span 28 county-level units during 2005–2024 [8].

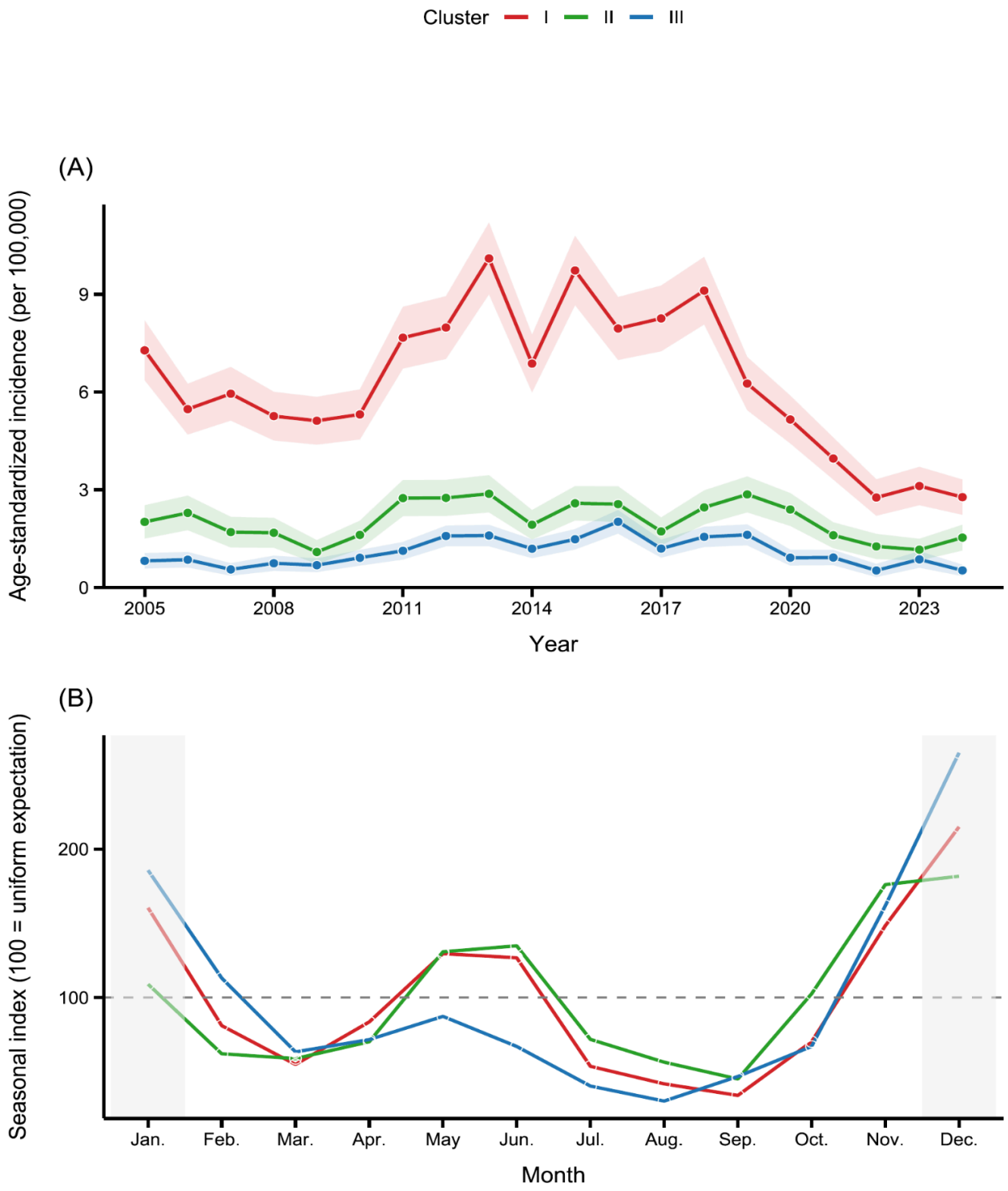


Figure 2

Long-term HFRS incidence trends and seasonality by endemic cluster.

Legend: Age-standardized incidence rate trends and seasonal index of HFRS across the three endemic clusters, Jiangxi Province, China, 2005–2024.

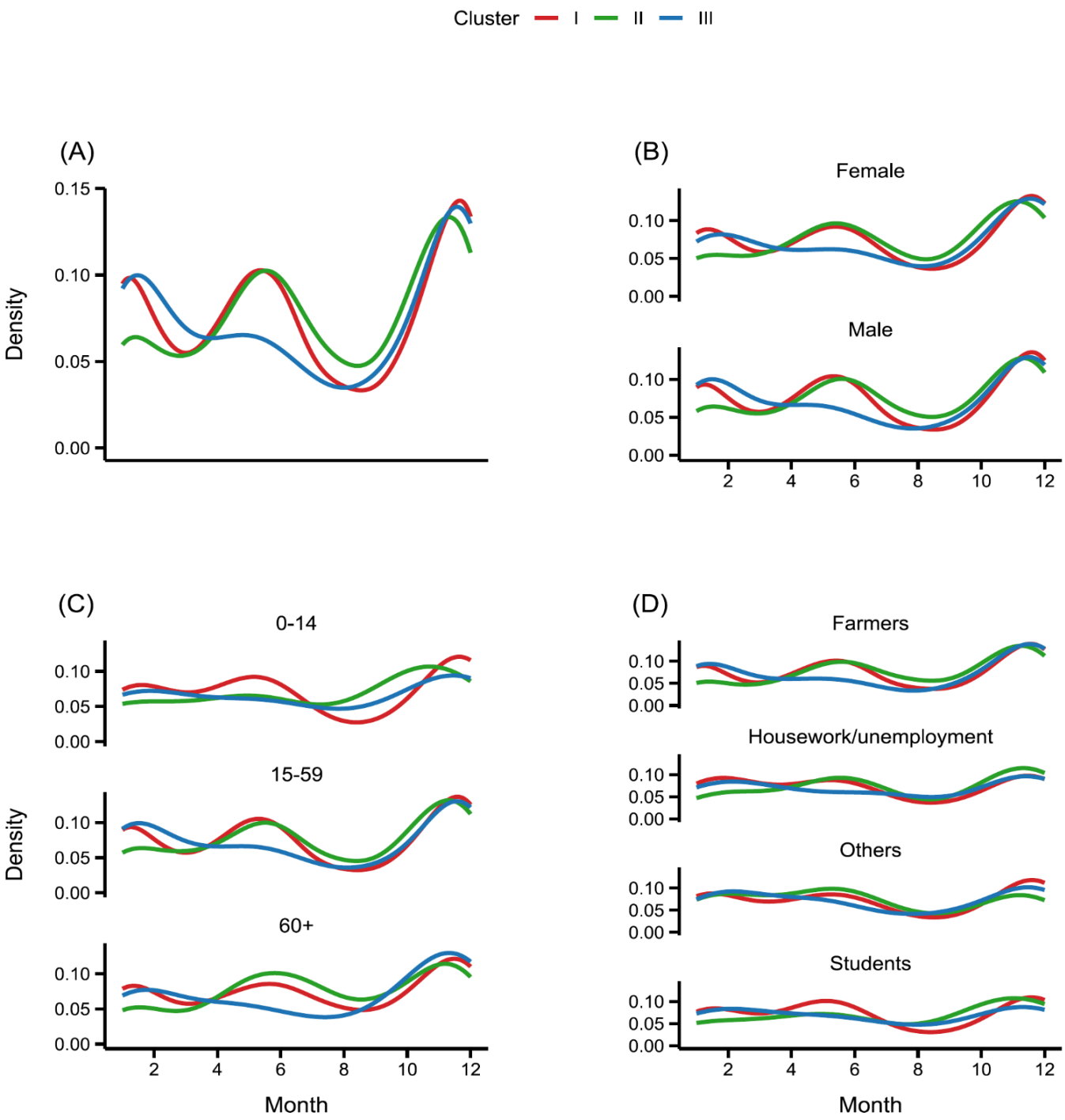


Figure 3

Monthly HFRS case density by demographic subgroup and endemic cluster.

Legend: Kernel-density plots of illness-onset month among reported HFRS cases, stratified by age group, sex, and occupation across the three endemic clusters, Jiangxi Province, China, 2005–2024.

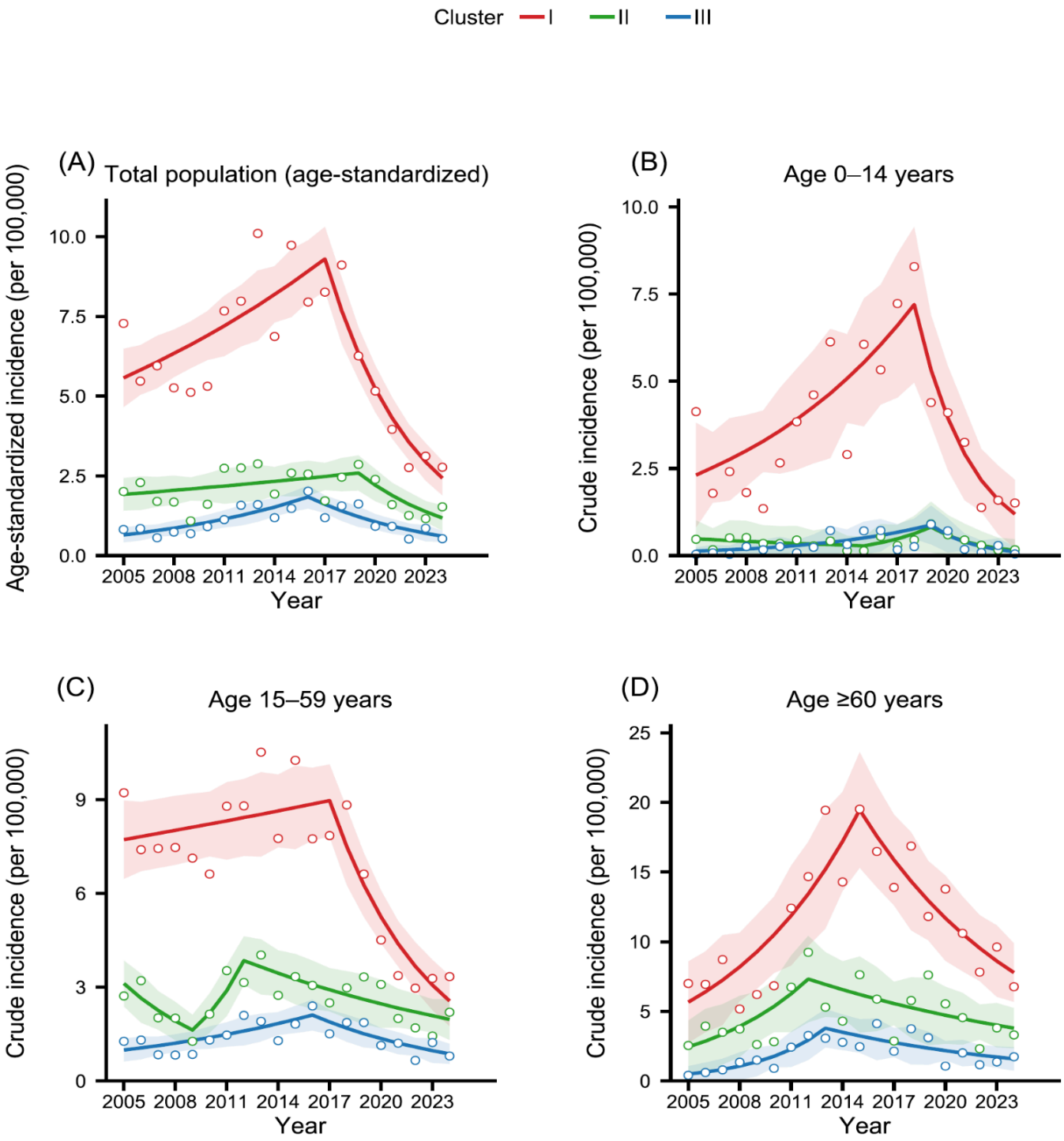


Figure 4

Joinpoint trends in HFRS incidence by cluster.

Legend: Open circles show observed annual rates; solid lines show Joinpoint fitted trends; and shaded ribbons show 95% confidence intervals. Age-standardized incidence is shown for the total population and age-specific incidence for the three age groups, Jiangxi Province, China, 2005–2024.

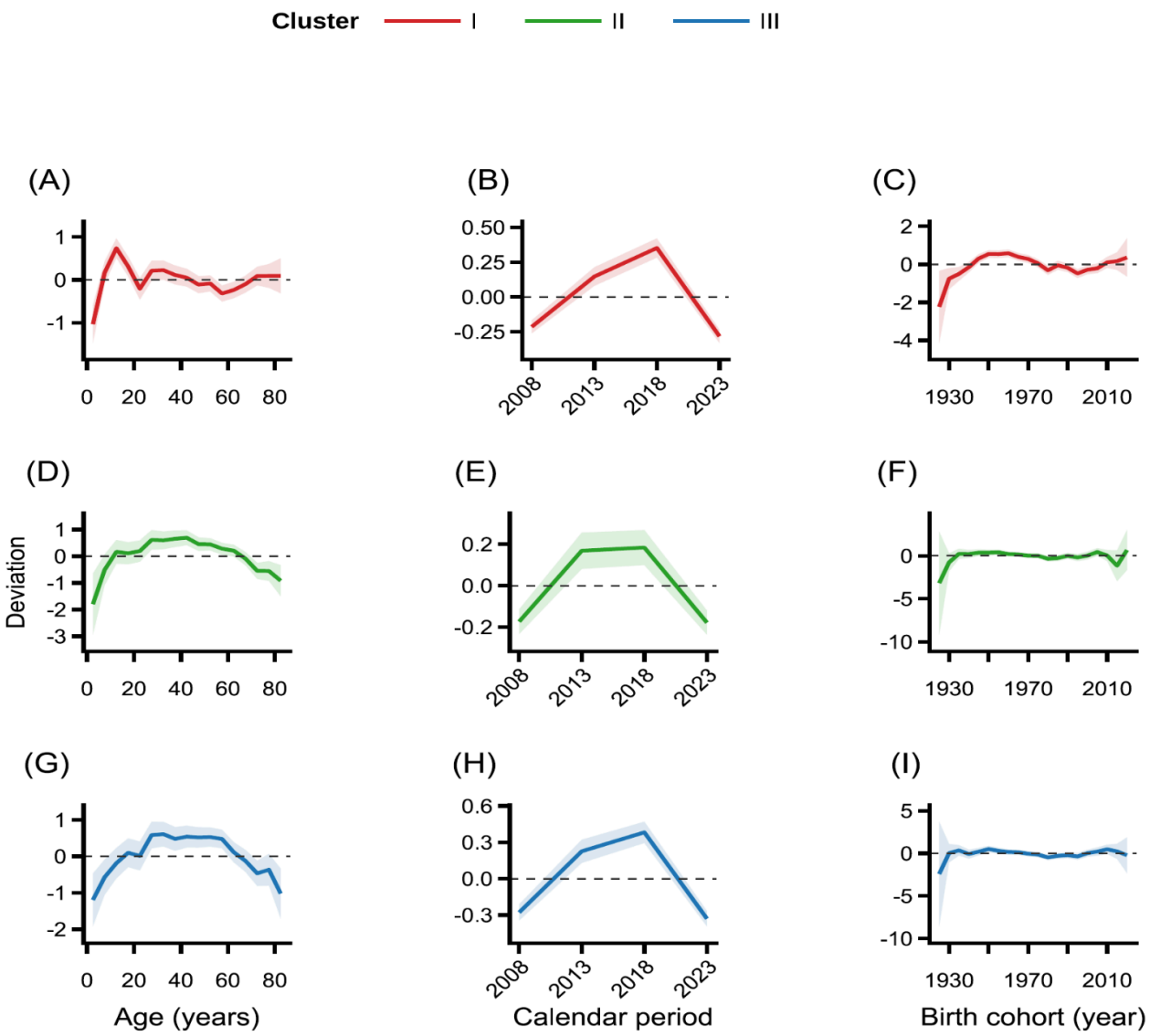


Figure 5

Age–period–cohort patterns in HFRS incidence by endemic cluster.

Legend: Intrinsic-estimator APC effects for the three clusters. Panels A–C, D–F, and G–I correspond to Cluster I (red), Cluster II (green), and Cluster III (blue), respectively. Each row shows deviations of age, period, and cohort effects from the reference, with 95% confidence intervals and a dashed line at zero.

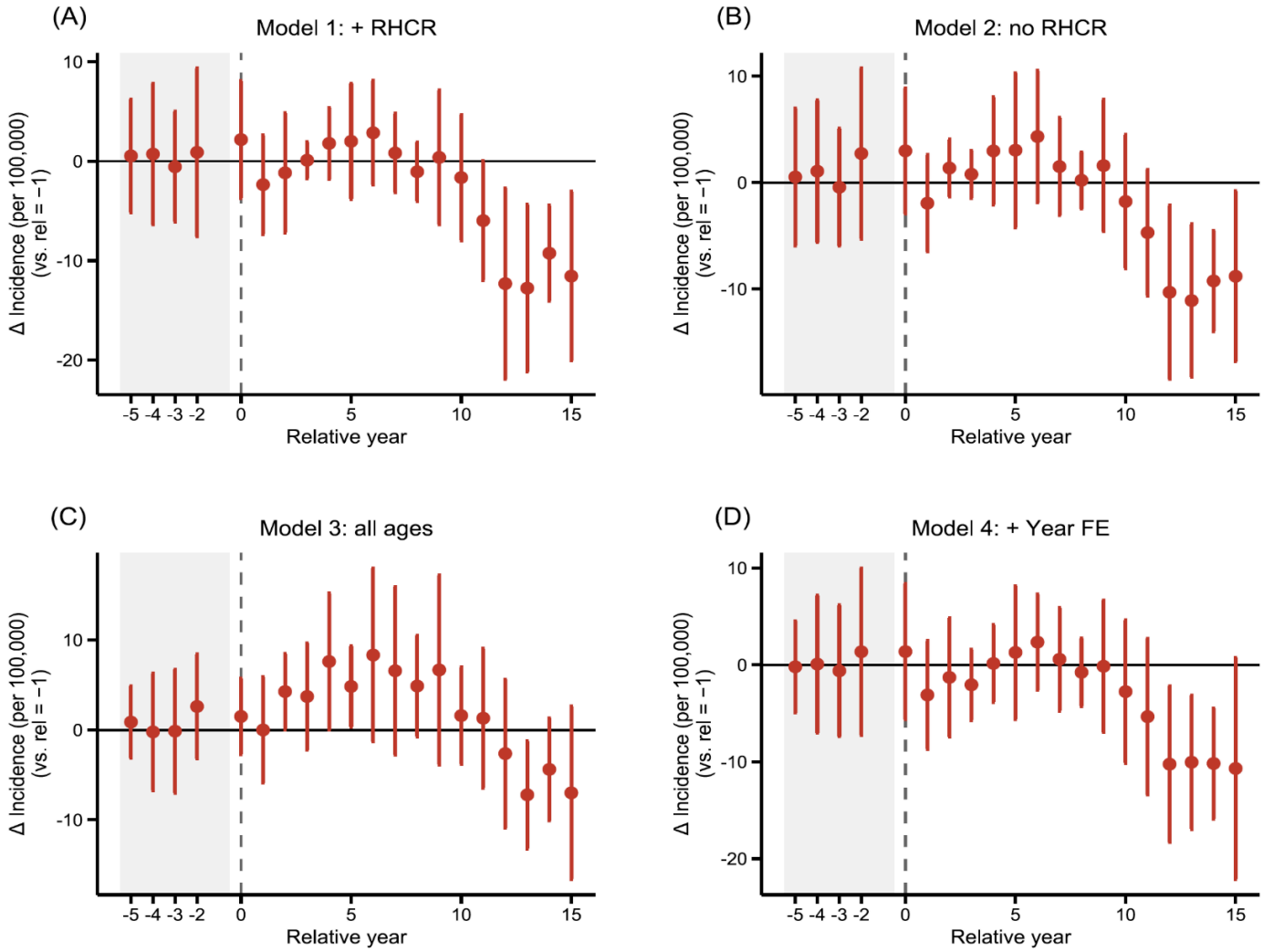


Figure 6

Event-study estimates after HFRS vaccination-programme initiation.

Legend: Incidence (per 100,000) in Cluster I (eight counties), Jiangxi Province, 2005–2024. Panel A: preferred specification (ages 15–59 years, adjusted for rodent carriage rate). Panel B: ages 15–59 years without rodent control. Panel C: pooled age-stratum specification (0–14, 15–59, and ≥60 years) with age-stratum fixed effects. Panel D: ages 15–59 years with year fixed effects. Shaded area: pre-implementation period (rel < 0). Dashed vertical line: rel = 0. Error bars: 95% confidence intervals with county-clustered standard errors. The y-axis shows the difference in incidence relative to rel = −1.

Supplementary Files

This is a list of supplementary files associated with this preprint. Click to download.

- TableS1.docx

- TableS5.docx
- TableS4.docx
- TableS3.docx
- TableS2.docx
- TableS6.docx
- FigureS4.pdf
- FigureS5.pdf
- FigureS3.pdf
- FigureS1.pdf
- FigureS2.pdf
- FigureS6.pdf
- AdditionalfilesLegends.docx